Development of a highly selective *Plasmodium falciparum* proteasome inhibitor with anti-malaria activity in humanized mice

Wenhu Zhan[#][a], **Hao Zhang**[#][a], **John Ginn**[#][b], **Annie Leung**[c], **Yi J. Liu**[c], **Mayako Michino**[b], **Akinori Toita**[b], **Rei Okamoto**[b], **Tzu-Tshin Wong**[b], **Toshihiro Imaeda**[b], **Ryoma Hara**[b], **Takafumi Yukawa**[b], **Sevil Chelebieva**[d], **Patrick K. Tumwebaze**[e], **Maria Jose Lafuente-Monasterio**[f], **Maria Santos Martinez-Martinez**[f], **Jeremie Vendome**[g], **Thijs Beuming**[g], **Kenjiro Sato**[b], **Kazuyoshi Aso**[b], **Philip J. Rosenthal**[h], **Roland A. Cooper**[d], **Peter T. Meinke**[b], **Carl F. Nathan**[a], **Laura A. Kirkman**[c], **Gang Lin**[a]

[a]Department of Microbiology & Immunology Weill Cornell Medicine 1300 York Ave, New York, NY 10065, USA [b]Tri-Institutional Therapeutics Discovery Institute 413 E 69th St, New York, NY 10065, USA [c]Department of Medicine, Division of Infectious Diseases Weill Cornell Medicine 1300 York Ave, New York, NY 10065, USA [d]Department of Natural Sciences and Mathematics Dominican University of California San Rafael, CA 94901, USA [e]Infectious Diseases Research Collaboration, Kampala, Uganda [f]Diseases of the Developing World (DDW) Tres Cantos Medicine Development Campus, GlaxoSmithKline Severo Ochoa 2, 28760, Tres Cantos, Madrid, Spain [g]Schrödinger, Inc. New York, NY 10036, USA [h]Department of Medicine University of California San Francisco, CA 94143, USA

[#] These authors contributed equally to this work.

Abstract

Plasmodium falciparum proteasome (Pf20S) inhibitors are active against *Plasmodium* at multiple stages – erythrocytic stages, gametocyte stages, liver stages and gamete activation, indicating that selective Pf20S inhibitors possess the potential to be therapeutic, prophylactic and transmission-blocking antimalarials. Starting from a reported compound, we developed a noncovalent, macrocyclic peptide inhibitor of the malarial proteasome with high species selectivity and improved pharmacokinetic properties. The compound demonstrates specific, time-dependent inhibition of the β5 subunit of the *Plasmodium falciparum* proteasome, kills artemisinin-sensitive and artemisinin-resistant *P. falciparum* isolates in vitro and reduces parasitemia in humanized, *P. falciparum*-infected mice.

Graphical Abstract
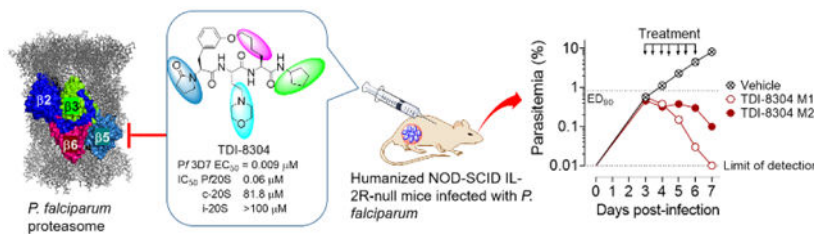
gal2005@med.cornell.edu, lak9015@med.cornell.edu.

Pf20S inhibitors possess the potential to be therapeutic, prophylactic and transmission-blocking antimalarials. We present a novel and highly species-selective malaria proteasome inhibitor that potently reduced parasitemia in humanized mice infected with *P. falciparum*, the most deadly plasmodium parasites.

Keywords

malaria; proteasome; inhibitor; selectivity; therapy

The spread of drug resistance threatens recent gains in malaria control even as the current burden of disease remains intolerable, with 228 million new cases and 405,000 deaths, primarily in children, estimated in 2018.[1] The limited range of clinically validated antimalarial targets and the danger of increasing resistance to current antimalarial regimens highlight the need for novel antimalarial agents. Proteasomes of pathogens have recently become targets of interest in tuberculosis, malaria, Chagas disease, leishmaniasis and schistosomiasis. The *Plasmodium falciparum* proteasome (Pf20S) has served as a promising target for parasite-selective proteasome inhibitors acting against erythrocytic, gametocyte, liver and mosquito stages, indicating that Pf20S inhibitors can potentially have therapeutic, prophylactic and transmission-blocking indications.[2] Given that human hematopoietic cells, plasma cells and plasmacytoid dendritic cells are highly susceptible to proteasome inhibition,[3] proteasome inhibitors for treatment of malaria must be highly selective for the malarial proteasome over the three proteolytic subunits of the human constitutive proteasome (c-20S) and the three proteolytic subunits of the human immunoproteasome (i-20S) to avoid toxicity and interference with immune responses.

We recently reported noncovalent Pf20S inhibitors that showed marked antimalarial activity against multiple stages of the parasites' life cycle.[2d, 4] However, these inhibitors all demonstrated fast clearance in vivo (Figure S1). To identify a compound for use in mouse proof of concept studies, we explored an alternative scaffold for Pf20S-selective inhibitors. Bogyo and coworkers recently reported a macrocyclic peptide, compound 1, that shows potent proteasome inhibition, selectivity and effective antimalarial activity.[5] However, compound 1 suffers from poor solubility and fast clearance by liver microsomes (Table S1).

We conducted an extensive structure-activity relationship (SAR) study to improve the pharmacokinetic properties of this scaffold (Figure 1). The full SAR study will be described in a separate paper. In brief, starting from compound 1, we first explored substitution at P5 to reduce hydrogen bond donor count and improve passive permeability, which yielded compound 2. Compound 2 is highly potent against *P. falciparum* strain Pf 3D7 (EC_{50} 1 nM)

and has activity against c-20S (IC_{50} 0.34 μM) and i-20S (IC_{50} > 34 μM) (Figure 1). However, the poor solubility and mouse microsomal stability of compound 2 needed additional optimization. Substitutions at P1, P3, and the tether were structure-guided using a docking workflow where macrocycles underwent extended conformation sampling followed by docking with a constraint to align the core of the query molecule with that of a reference pose model.[6] This pose model for the macrocycle series in Pf20S was initially developed for Compound 2 based on the acyclic analog bound in the yeast proteasome crystal structure (PDB: 3MG4) (Figure 2).[7] This docking workflow was implemented into LiveDesign for automated docking pose generation. We modified the P3 moiety to reduce LogD by replacing the phenyl with a morpholino group, and further modified the P1 moiety to reduce a lability to hydrolysis by replacing 2,2,2-trifluoroethylamino with cyclopropylmethyl, yielding compound 3. Compound 3 showed a comparable EC_{50} against *P falciparum* and demonstrated improved selectivity for c-20S (Figure 1). This optimization also improved metabolic stability and solubility (> 130 μg/mL). Further improvements in metabolic stability were realized by substitution at P1 with a cyclopentyl moiety and replacement of the biaryl ether with a mono phenyl alkyl chain. The final compound, TDI-8304, was highly potent against Pf 3D7 with marked selectivity for inhibition of Pf20S over human proteasomes (Figure 3A).

To determine the inhibition modality of TDI-8304, we monitored the hydrolysis of the proteasome substrate suc-LLVY-AMC by Pf20S in the presence of 0.5 μM β2-specific inhibitor WLW-VS and TDI-8304 at indicated concentrations (Figure 3B). TDI-8304 demonstrated time-dependent inhibition with an induced-fit mechanism.[8] The hyperbolic correlation of k_{obs} as a function of TDI-8304 concentrations was fit to equation $k_{obs} = k_6 + (k_5 / (1 + (K_i^{app} / [I]))$ and the values of K_i^{app} 1,007 nM, K_i^{*app} 89.6 nM and $t_{1/2}$ 14.4-minute half-life for the Pf20S:TDI-8304 complex were calculated by equation $K_i^* = K_i / (1 + K_5 / k_6)$ (Figure 3C). TDI-8304 dose-dependently blocked labelling of Pf20S β5, but not of Pf20S β1 or β2 (Figure 3D), by MV151, suggesting that TDI-8304 is a highly specific inhibitor of Pf20S β5.

TDI-8304 is nontoxic to HepG2 cells (Figure 4A) and potent not only against *Pf* 3D7 (Figure 4A) but also against the *P. falciparum* lab strain Dd2 and two Dd2-derived strains that are resistant to our previous noncovalent proteasome inhibitors PKS21004 and TDI4258 by virtue of mutation Pf20Sβ6A117D in the adjacent β6 subunit (which changes the conformation of S3 and S4 binding pockets of the β5 active site) and mutation Pf20Sβ5A49S in the active site of the β5 catalytic domain, respectively.[2d, 4] The EC_{50} values of TDI-8304 against Dd2 and Dd2β5A49S were comparable, suggesting that its binding mode, which is stabilized by its macrocyclic tether structure, is unaffected by the mutation. However, an ~18-fold reduction in potency against Dd2β6A117D (Figure 4B) suggests that the conformational changes caused by the β6A117D mutation affect the binding of TDI8304 more than the conformational changes caused by the β5A49S mutation. Supporting on-target whole-cell activity, a 6-hour exposure to TDI-8304 led to accumulation of polyubiquitinated proteins in *Pf* trophozoites (Figure 4C). TDI-8304 showed comparable activity against *Pf* strains HB3 (chloroquine-sensitive), 3663 (ART-sensitive) and 4884 (ART-resistant)[9] (Figure 4D), indicating no apparent cross-resistance.

TDI-8304 was further tested for ex vivo activity against fresh *falciparum* isolates from 38 malaria patients in Uganda. The EC_{50}s ranged from 5–30 nM, with a mean of 18 nM, in agreement with the results from *P. falciparum* laboratory strains (Figure 4E). There was no observed association between sensitivities to TDI-8304 and chloroquine resistance among the clinical isolates.

Several studies have established that proteasome inhibitors are synergistic with ARTs. [2a, 2b, 2d] To investigate the synergy of TDI-8304 with ART, we tested TDI-8304 in combination with dihydroartemisinin (DHA) using a modified ring-stage survival assay (RSA) with both artemisinin-sensitive *Pf*Cam3.I[Rev] and artemisinin-resistant *Pf* Cam3.I[R539T] in a multidrug-resistant Dd2 strain background. We exposed early (1- to 3-h) ring-stage parasites to a 3-h pulse of DHA and continuous TDI-8304 for further 69 h, as described.[2d] Parasitemia was measured at 72 h post initial exposure. Isobologram analyses clearly demonstrated synergistic killing of artemisinin–sensitive (Figure 4F Left) and artemisinin-resistant (Figure 4F right) parasites by the combination of TDI-8304 and DHA.

TDI-8304 is metabolically stable upon incubation with human, mouse and rat microsomes and cell-permeable (Figure 5A). It inhibited by less than 10% a panel of CYP enzymes, and showed no cytotoxicity to HepG2 cells. TDI-8304 further showed no inhibition of the hERG (Ether-à-go-go) channel, implying low risk of cardiac arrhythmia through action on this ion channel. TDI-8304 is rapidly cleared when administered to mice by *i.v.* (Figure 5B) or *p.o.* routes (Figure S1), but shows prolonged clearance when administered *s.c.* (Figure 5B). This allowed twice-daily dosing (b.i.d) to afford sufficient exposure for efficacy experiments in mice. We tested TDI-8304 in a humanized mouse model of Pf infection[10] with *s.c.* administration at 100 mg/kg b.i.d., from days 3 – 6 post infection and monitoring parasitemia from day 3 until day 7 (Figure 5C). TDI-8304 reduced the parasitemia by a factor of 2 log10 in one mouse and cleared the parasitemia in another mouse. Pharmacokinetics of TDI-8304 from the infected SCID mice during the course of the assay were also determined (Table S2), and the data showed that the whole blood concentration of TDI-8304 was constantly greater than the EC_{90} (29 nM) of TDI-8304 in both mice, except for one data point at the 24h time-point in mouse 2 (Figure S2), in agreement with the observed reduction of parasitemia in infected mice.

In conclusion, we developed a preclinical and species-selective *P. falciparum* proteasome inhibitor with marked antimalarial activity in a humanized mouse model of *P. falciparum* infection. To our knowledge, this is the first noncovalent Pf20S inhibitor shown to have anti-malaria activity in *Pf* infected mice.

Supplementary Material

Refer to Web version on PubMed Central for supplementary material.

Acknowledgements

References

[1]. WHO, World Health Organization, Geneva: World Health Organization, 2018.

[2]. a)Dogovski C, Xie SC, Burgio G, Bridgford J, Mok S, McCaw JM, Chotivanich K, Kenny S, Gnadig N, Straimer J, Bozdech Z, Fidock DA, Simpson JA, Dondorp AM, Foote S, Klonis N, Tilley L, PLoS Biol 2015, 13, e1002132; [PubMed: 25901609] b)Li H, O'Donoghue AJ, van der Linden WA, Xie SC, Yoo E, Foe IT, Tilley L, Craik CS, da Fonseca PC, Bogyo M, Nature 2016, 530, 233; [PubMed: 26863983] c)Zhang M, Wang C, Otto TD, Oberstaller J, Liao X, Adapa SR, Udenze K, Bronner IF, Casandra D, Mayho M, Brown J, Li S, Swanson J, Rayner JC, Jiang RHY, Adams JH, Science 2018, 360;d)Kirkman LA, Zhan W, Visone J, Dziedziech A, Singh PK, Fan H, Tong X, Bruzual I, Hara R, Kawasaki M, Imaeda T, Okamoto R, Sato K, Michino M, Alvaro EF, Guiang LF, Sanz L, Mota DJ, Govindasamy K, Wang R, Ling Y, Tumwebaze PK, Sukenick G, Shi L, Vendome J, Bhanot P, Rosenthal PJ, Aso K, Foley MA, Cooper RA, Kafsack B, Doggett JS, Nathan CF, Lin G, Proc Natl Acad Sci U S A 2018, 115, E6863–E6870. [PubMed: 29967165]

[3]. a)Hirai M, Kadowaki N, Kitawaki T, Fujita H, Takaori-Kondo A, Fukui R, Miyake K, Maeda T, Kamihira S, Miyachi Y, Uchiyama T, Blood 2011, 117, 500; [PubMed: 20956804] b)Neubert K, Meister S, Moser K, Weisel F, Maseda D, Amann K, Wiethe C, Winkler TH, Kalden JR, Manz RA, Voll RE, Nat Med 2008, 14, 748; [PubMed: 18542049] c)Santos R. d. L. A., Bai L, Singh PK, Murakami N, Fan H, Zhan W, Zhu Y, Jiang X, Zhang K, Assker JP, Nathan CF, Li H, Azzi J, Lin G, Nat Commun 2017, 8, 1692. [PubMed: 29167449]

[4]. Zhan W, Visone J, Ouellette T, Harris JC, Wang R, Zhang H, Singh PK, Ginn J, Sukenick G, Wong TT, Okoro JI, Scales RM, Tumwebaze PK, Rosenthal PJ, Kafsack BFC, Cooper RA, Meinke PT, Kirkman LA, Lin G, J Med Chem 2019, 62, 6137. [PubMed: 31177777]

[5]. Li H, Tsu C, Blackburn C, Li G, Hales P, Dick L, Bogyo M, J Am Chem Soc 2014, 136, 13562. [PubMed: 25226494]

[6]. Sindhikara D, Spronk SA, Day T, Borrelli K, Cheney DL, Posy SL, J Chem Inf Model 2017, 57, 1881. [PubMed: 28727915]

[7]. Blackburn C, Gigstad KM, Hales P, Garcia K, Jones M, Bruzzese FJ, Barrett C, Liu JX, Soucy TA, Sappal DS, Bump N, Olhava EJ, Fleming P, Dick LR, Tsu C, Sintchak MD, Blank JL, Biochem J 2010, 430, 461. [PubMed: 20632995]

[8]. Copeland RA, in Evaluation of enzyme inhibitors in drug discovery: A guide for medicinal chemists and pharmacologists, Second Edition ed., John Wiley & Sons, Inc., Hoboken, 2013.

[9]. Ariey F, Witkowski B, Amaratunga C, Beghain J, Langlois AC, Khim N, Kim S, Duru V, Bouchier C, Ma L, Lim P, Leang R, Duong S, Sreng S, Suon S, Chuor CM, Bout DM, Menard S, Rogers WO, Genton B, Fandeur T, Miotto O, Ringwald P, Le Bras J, Berry A, Barale JC, Fairhurst RM, Benoit-Vical F, Mercereau-Puijalon O, Menard D, Nature 2014, 505, 50. [PubMed: 24352242]

[10]. Angulo-Barturen I, Jimenez-Diaz MB, Mulet T, Rullas J, Herreros E, Ferrer S, Jimenez E, Mendoza A, Regadera J, Rosenthal PJ, Bathurst I, Pompliano DL, Gomez de las Heras F, Gargallo-Viola D, PLoS One 2008, 3, e2252. [PubMed: 18493601]
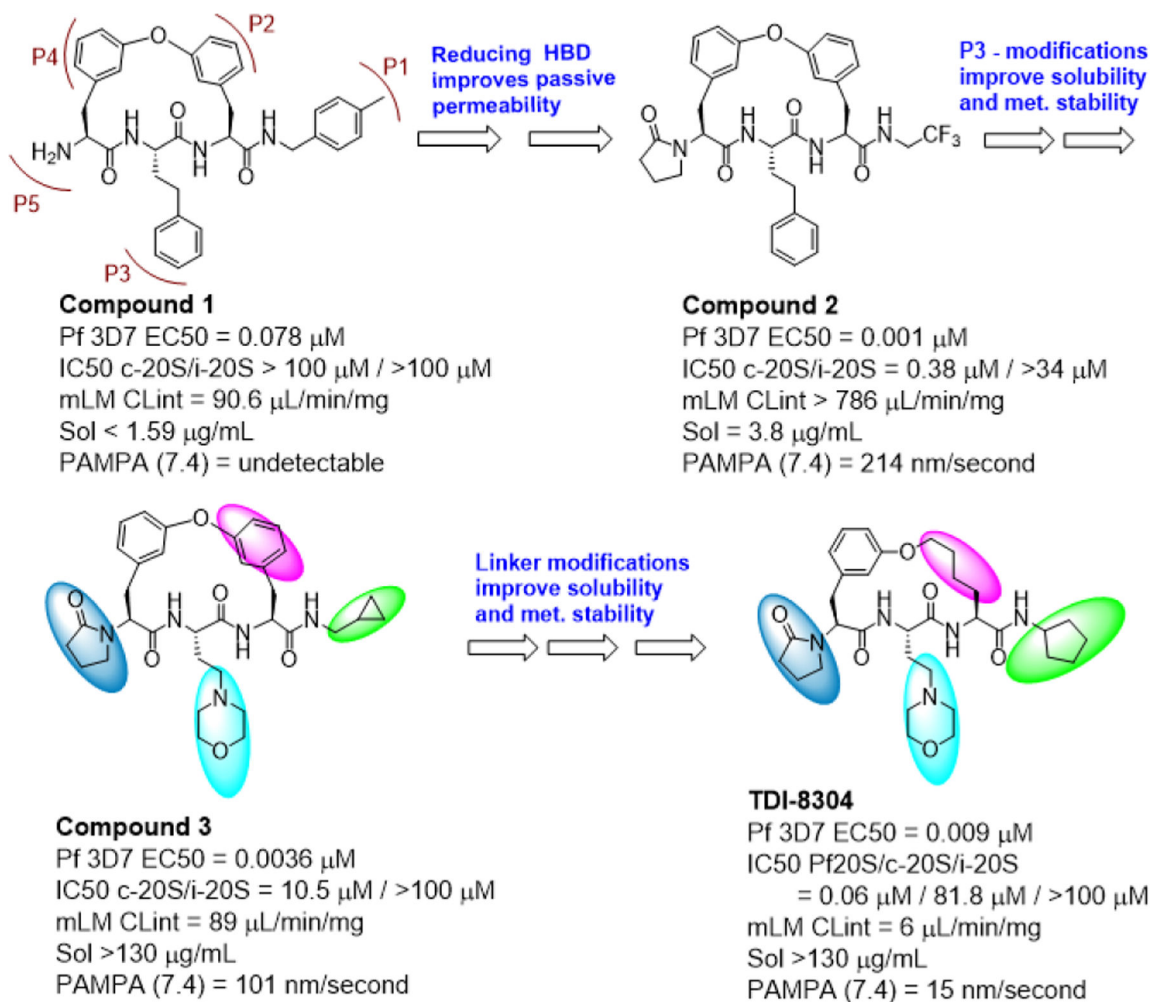
Figure 1.
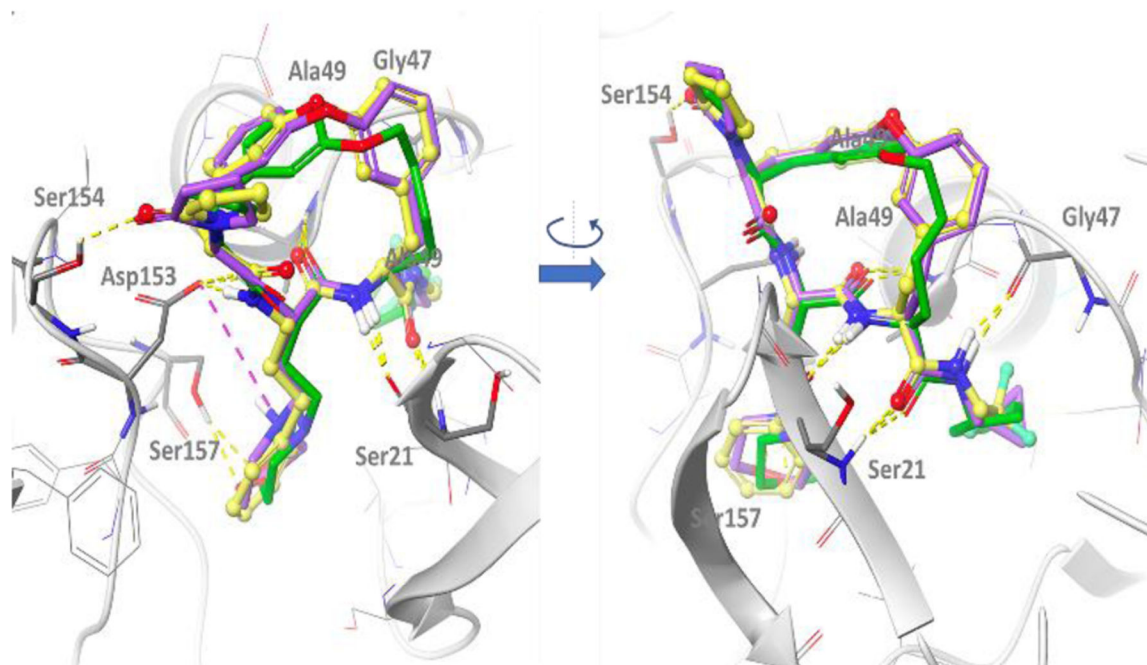SAR evolution from compound 1 to TDI-8304.

Figure 2.
Docking model of macrocyclic peptides in Pf20S. The structure of Pf20S β5–6 was obtained by homology modeling based on yeast 20S β5–6 (3MG4), and then refined using molecular dynamics simulations. The amide bonds of all compounds form 5 well conserved hydrogen bonds with the backbone of Ser21, Gly47 and Ala49 as well as the side chain of Asp153. Additionally, the pyrrolidone in P5 of compounds 2, 3 and TDI-8304 forms a hydrogen bond with Ser154, and the morpholino oxygen in compound 3 and TDI-8304 form a hydrogen bond with hydroxyl group of Ser157 in β6. For compound 3, the protonated form of the morpholine has been represented to illustrate the possible salt bridge with Asp153, but the neutral form might predominate at relevant pH (predicted pKa ~ 6.6). Compound 2 is shown in yellow, compound 3 in purple and TDI-8304 in green.
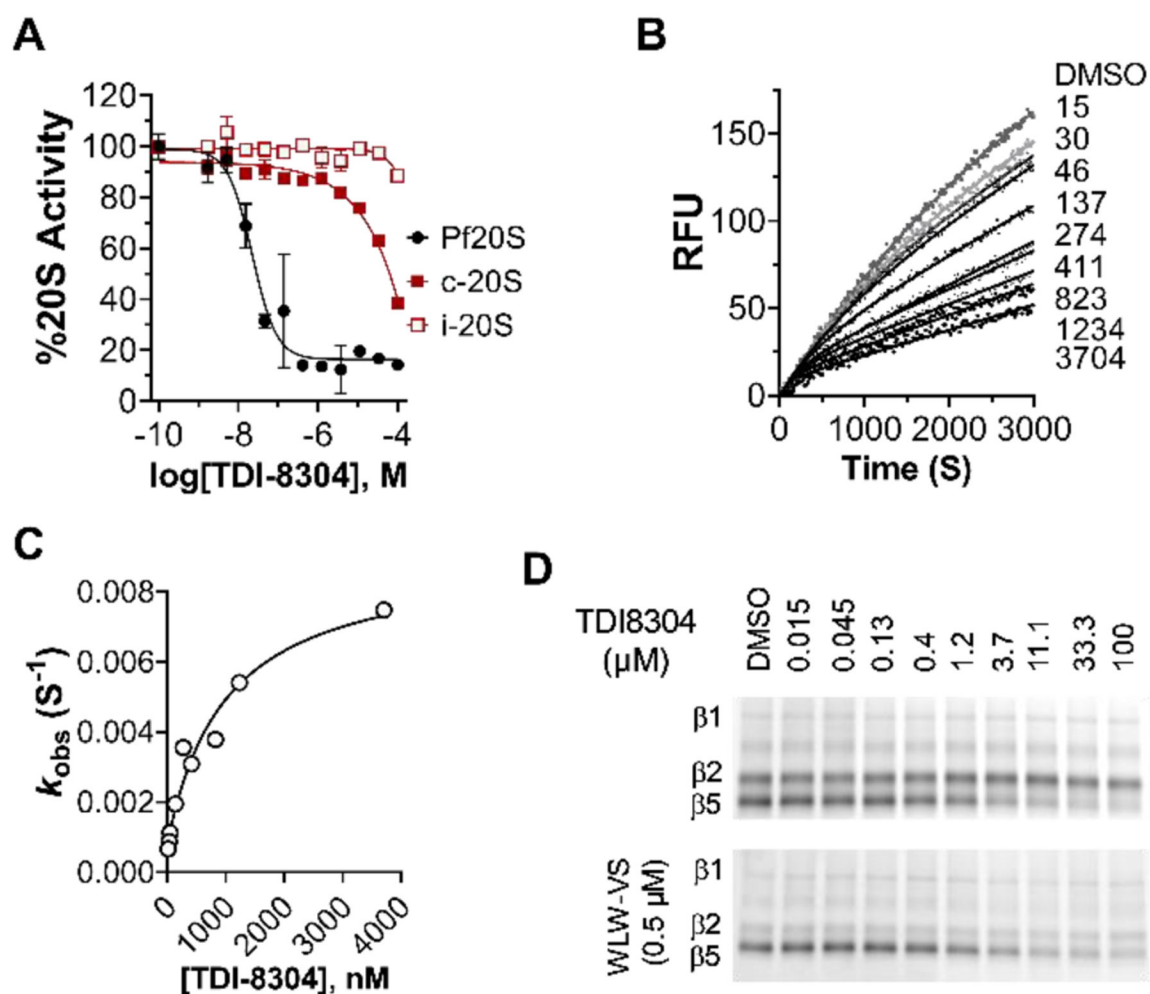
Figure 3.
TDI-8304 selectively inhibits Pf20S. A) Dose-dependent inhibition of chymotryptic β5 subunits of Pf20S, human c-20S and i-20S. B) Time courses of inhibition of Pf20S β5 by TDI-8304 at indicated concentrations (nM). C) Plot of k_{obs} values obtained from the time course curves with varied TDI-8304 concentrations yields K_I^{app} = 1007 nM, K_i^* = 89.6 nM and k_{off} = 0.0008 S^{-1}. D) TDI-8304 specifically inhibited Pf20S β5 but not β2 or β1, from being labeled by MV151, either in the absence of a Pf20S β2 specific inhibitor WLW-VS[3] (top) or in the presence of WLW-VS (bottom).
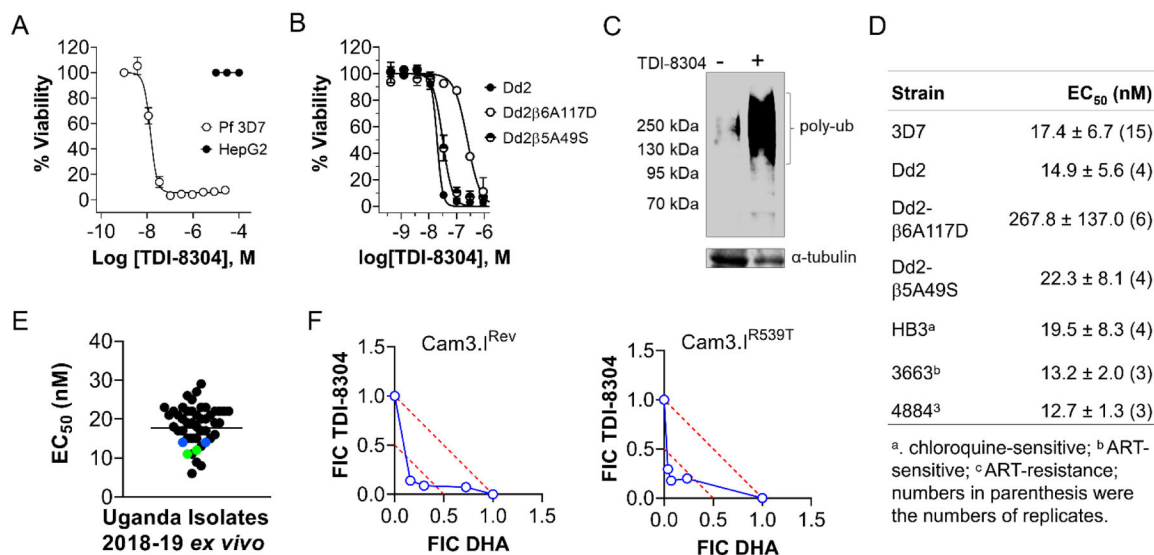
Figure 4.

TDI-8304 inhibits growth of erythrocytic stage *P. falciparum*. A) TDI-8304 potently inhibited Pf3D7 growth (open black circles) but is not cytotoxic for HepG2 human hepatoma cells (solid black circles); B) TDI-8304 inhibits growth of Pf Dd2 and two proteasome inhibitor-resistant strains, Pf Dd2β6A117D and Pf Dd2β5A49S. C) TDI-8304 at 1 μM led to accumulation of polyubiquitinated proteins after treatment of *P. falciparum* schizonts for 6 hours. D) EC_{50} values of TDI-8304 against *P. falciparum* strains with various drug resistance profiles; E) Ex vivo activity of TDI-8304 against 38 clinical isolates from Uganda in years 2018 and 2019. The geometric mean EC_{50} was 18 nM. Each black spot represents a single *P. falciparum* isolate. Blue and green spots represent Dd2 and 3D7 laboratory controls, respectively. F) In vitro synergy of TDI-8304 and DHA against artemisinin-sensitive *P. falciparum* Dd2 Cam3.I[Rev] and artemisinin-resistant Cam3.I[R539T]. Data were average of two independent experiments and each in duplicates. FIC: fractional inhibitory concentration.

A

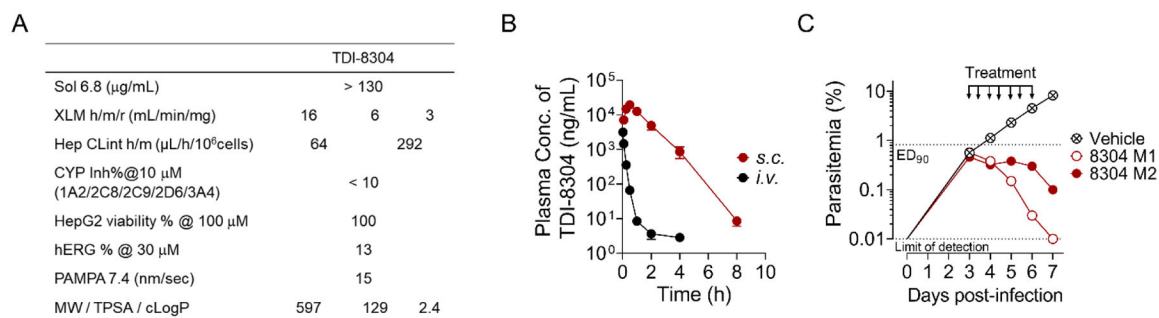|	TDI-8304		
Sol 6.8 (µg/mL)	> 130		
XLM h/m/r (mL/min/mg)	16	6	3
Hep CLint h/m (µL/h/10⁶cells)	64		292
CYP Inh%@10 µM (1A2/2C8/2C9/2D6/3A4)	< 10		
HepG2 viability % @ 100 µM	100		
hERG % @ 30 µM	13		
PAMPA 7.4 (nm/sec)	15		
MW / TPSA / cLogP	597	129	2.4

Figure 5.

Pharmacokinetic properties of TDI-8304 and its efficacy in humanized, *P. falciparum*-infected mice. A) PK properties of TDI-8304. B) In vivo PK of TDI-8304 administrated *i.v.* (1 mg/kg) or *s.c.* (100 mg/kg). C) Parasitemia reduction of *P. falciparum* $Pf3D7^{0087/N9}$ in NOD-SCID IL-2R-null mice transfused with human erythrocytes. TDI-8304 was given twice-daily by s.c. (100 mg/kg) on days 3 through 6. Two mice were used in each group, each serially sampled on days 3 to 7. Percentage parasitemia was calculated by acquiring a minimum number of 500 parasitized erythrocytes.